

Profiles and Polarization Properties of Emission Lines from Relativistic Disks

Jun OGURA, Nobuyori OHUO *, and Yasufumi KOJIMA

Department of Physics, Hiroshima University, Higashi-Hiroshima 739-8526

E-mail(JO):ogura@theo.phys.sci.hiroshima-u.ac.jp

(Received 2000 January 20; accepted 2000 July 10)

Abstract

We examined the profiles and polarization properties of emission lines originating from the extremely relativistic region of Kepler disks. Because the emission region is more localized to the inner part, e.g., a few times the black hole radius, the profiles, and polarization properties are remarkably modified. The black hole spin significantly affects the properties through the inner edge. This observation, in spite of the technical difficulties, provides an important diagnostic of the relativistic region.

Key words: black hole physics — line: profiles — polarization

1. Introduction

In recent years, the evidence of black holes has become more apparent owing to X-ray astronomy. Some broad iron lines from Seyfert galaxies were detected and attributed to relativistic effects in the emission region (Tanaka et al. 1995; Iwasawa et al. 1996; Nandra et al. 1997). The lines emitted from accretion disks near the central black hole show broad asymmetric profiles, significantly modified by both the gravitational redshift and Doppler effects. The emission region is inferred to be located near several times the black hole horizon, since the line width determines the strength of the relativistic effect, i.e., the radius from the disk center. Strong gravitational effects are crucial there, and the angular momentum of a rotating black hole is also constrained. (Dabrowski et al. 1997; Weaver, Yaqoob 1998)

The theoretical possibility was discussed beforehand. Fabian et al. (1989) calculated the line profile emitted from accretion disks around non-rotating black holes. Kojima (1991) and Laor (1991) independently extended this study to rotating cases. The effect of black hole rotation appears only in the disk structure close to the central black hole. The present remarkable observation gives not only evidence, but also the property of the central black holes. Future observations will give new topics related to strong gravitational phenomena.

Some natures of central black holes, which will be observable by the next advanced technique, are also discussed. Reynolds et al. (1999) calculated an X-ray reverberation map of lines for flares on the disk, which constrains the mass and spin of the black hole. In addition

to the intensity and its time variation, the polarization of light is important. Polarization is expected to be produced by electron scattering above the accretion disk. Several authors (Connors et al. 1980; Laor et al. 1990) have discussed the possibility. In particular, polarization in the emission line may be important, although the observational technique is very difficult. The emission region of the line is inferred by the profile, so that the polarization is an additional diagnostic tool. Chen and Eardley (1991) already studied the polarization properties of the line originating from a disk around a Schwarzschild black hole. It is important to extend their calculation to a Kerr black hole and to explore the effect of the black hole rotation, since the current observation of the broad lines suggests likely rotating black holes. In this paper, we discuss a theoretical calculation of the possibility in advance, that is, the polarization and line profile originating from a disk around a Kerr black hole. In the next section, we describe our models. The line profiles and the polarizations depend on several parameters. In section 3, the numerical results are given to demonstrate typical examples. We show how additional information can be useful for determining the models. Section 4 is devoted to a discussion. We use the units $c = G = 1$ throughout the paper.

2. Assumptions and Calculation Methods

In this section, we briefly summarize our model and the numerical method. The details of the formalism are given elsewhere e.g., for the line profile (Kojima 1991) and the polarization (Connors et al. 1980).

The polarization of a beam of radiation can be described by the Stokes parameters (Chandrasekhar 1960),

* Present address: Institute for Hydrospheric-Atmospheric Sciences, Nagoya Univ., Nagoya 464-8601.

i.e., the intensity I , linear polarization parameters Q , U , and the circular parameter V . The circular parameter vanishes for polarization induced by scattering. These quantities are related to the degree of polarization, δ , and the angle of the plane of the polarization, ψ , as

$$\delta = \frac{\sqrt{Q^2 + U^2}}{I}, \quad \psi = \frac{1}{2} \tan^{-1} \left(\frac{U}{Q} \right). \quad (1)$$

For a purely electron-scattering atmosphere, the polarization is determined by the local physics. The degree of polarization depends on the emission angle, ϕ_e , which is measured in the rest frame. An explicit formula has been derived by Chandrasekhar (1960). The degree, δ_e , ranges from 12% for $\phi_e = 90^\circ$ (edge-on case) to 0 for $\phi_e = 0$ (face-on case).

These polarization quantities as well as the energy, E_{em} , in the rest frame of emitting matter are related to the observed ones by the null geodesics. The observed energy, E_{ob} , is shifted as $E_{\text{ob}} = gE_{\text{em}}$, with the redshift factor g^{-1} . Since the polarization degree, δ , is a scalar, we have the observed value as $\delta = \delta_e$, for the corresponding path. The angle of the polarization plane measured by an observer can be calculated by the parallel transportation along the null geodesics. The polarization vector at infinity can be constructed with the help of the so-called Walker–Penrose constant in the Kerr metric.

In this paper, we assume a geometrically thin, axisymmetric disk co-rotating in the equatorial plane around a Kerr black hole. The polarization is assumed to be produced by electron scattering in the disk surface ranging from R_{in} to R_{out} . We adopt a power law-form with a constant index, q , as the local specific intensity $[I_e(E_{\text{em}}, \phi_e, r_e)]$;

$$I_e(E_{\text{em}}, \phi_e, r_e) \propto \frac{\epsilon(\phi_e)}{4\pi} r^{-q} \delta(E_{\text{em}} - E_o), \quad (2)$$

where E_o is the rest energy of the line and $\epsilon(\phi_e)$ describes the local line specific intensity. We assumed that the intrinsic broadening of the line is so small that it can be neglected compared to the kinematical effect.

The flux by an observer at θ_o is calculated by integrating over the disk surface,

$$F_o(E, \theta_o) = \int \int g^3 I_e(E/g, \phi_e, r_e) d\Omega. \quad (3)$$

In a similar way, the observed net Stokes parameters \bar{Q} , \bar{U} are calculated as

$$\begin{aligned} & \bar{Q}_o(E, \theta_o) + i\bar{U}_o(E, \theta_o) \\ &= \int \int g^3 \delta_e (\cos 2\psi + i \sin 2\psi) I_e(E/g, \phi_e, r_e) d\Omega \end{aligned} \quad (4)$$

The observed degree, δ , and angle of polarization, ψ , are calculated by equation (1). The angle is measured from the direction perpendicular to both the normal vector of

the disk and the propagation vector of the light. These quantities depend on the disk inclination, θ_o , the model parameters q , R_{in} , R_{out} , and the Kerr parameter a . It is possible to calculate them in this large parameter space, but results are not easy to be understood. Since we found that the dependence of q is not very sensitive, the results for $q = 3$ are shown in the next section. As the outer boundary, R_{out} , of the disk increases, the relativistic effects are less prominent because of the average over the disk. We will show a representative result of $R_{\text{out}} = 20M$ in the next section. Here M is the mass of the central black hole.

3. Numerical Results

Before discussing the realistic cases, we illustrate the polarization angles emitted from a few rings in figure 1. Because the general cases can be regarded as a summation over a certain range of the disk, this figure is useful for understanding the relativistic effects. The shift in the energy and the polarization angle is small for emission from a ring of large radius. As the radius decreases, the range of the observed energy is more spread and the polarization angle significantly deviates from 90° . These quantities strongly depend on the emission position, and therefore give the information about the emission region as well as the line profile.

In figure 2-a and 2-b, we show the polarization angle and the degree of the emission line from the disk around a black hole. They are shown as a function of energy for three inclination angles of the disk. The other parameters are $R_{\text{in}} = 1.24M$, $R_{\text{out}} = 20M$, $q = 3$, and $a = 0.998M$. The inner radius, R_{in} , is chosen as a marginally stable radius of the Kepler disk around the rotating black hole with $a = 0.998M$. Each curve is drawn for the range of the shifted energy. The angles of these models significantly deviate from the value of 90° in a non-relativistic calculation. The deviation is very clear for a small inclination angle of the disk, although the polarization degree is small. The degree decreases with the decrease in the inclination angle. Indeed, the degree vanishes for the face-on case ($i = 0^\circ$), since the degree is zero for the radiation perpendicular to the disk surface, as discussed in the previous section.

In figure 3, we compared the emission from three models in the line profile, the polarization angle and the degree. The three models are different in the inner boundary, which is chosen as the radius of the marginally stable orbit around the black hole. That is, $R_{\text{in}} = 6M$ for $a = 0$, and $R_{\text{in}} = 1.24M$, $a = 0.998M$. We also show the case of $R_{\text{in}} = 6M$, $a = 0.998M$ for a comparison. As shown in previous calculations of the line profiles, the effect of black hole rotation appears through the inner boundary. This is also true for the polarization. Two models with the same innermost radius, $R_{\text{in}} = 6M$, give

almost the same result, which is consistent with Kojima (1991). The effect of the innermost point is clear in only the red-shifted part.

The results mentioned so far are important for the idealized situation, since the spectro-polarimetry of the line is a quite difficult challenge in future observations. We consider the energy-integrated values, which are useful for an observation without spectro-polarimetry. The polarization angle and the degree for energy-integrated line photons are shown in figure 4. The relativistic effects significantly appear in both of polarization angle and the degree for any inclination angle.

Finally, we will apply our model to the broad iron line discovered in the Seyfert galaxy MCG-6-30-15. From the line profile, some parameters are inferred (Nandra et al. 1997), but inconclusive. The present data fit equally well with rotating and non-rotating black hole models. Using their fitting parameters, we show the polarization properties as well as the line profile in figure 5. The difference between the rotating and non-rotating models is evident in the redshift part. The polarization will indeed give additional information, although the model parameters will not be uniquely determined.

4. Discussion

Chen and Eardley (1991) calculated the profile and the polarization property of the line emitted for the mildly relativistic case, in particular, their calculation is limited to a non-rotating black hole. We extend their work to the extremely relativistic case with the rotating black hole, since recent observations suggest evidence of relativistic phenomena at a few times the black hole radius. In such a region of strong gravitational field, the black hole spin is important, since the inner edge of the disk depends on it. Our calculations show that the difference in black holes, i.e., spin effect, appears through the possible range of emission. Future observations, despite the difficulties, may produce phenomena relevant to our model.

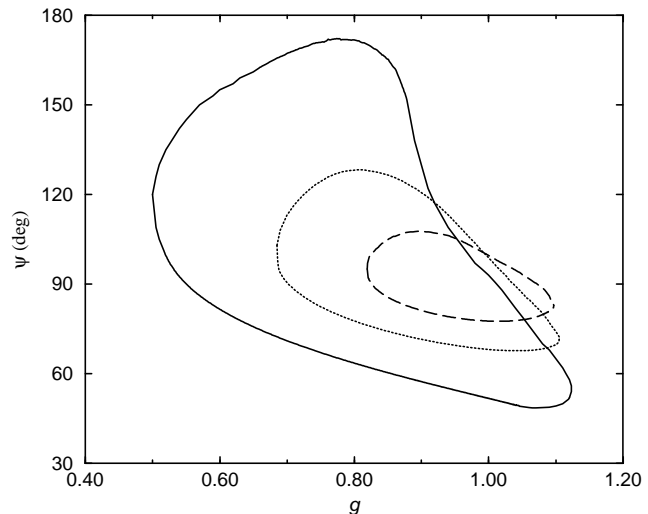


Fig. 1.. Polarization angle emitted from rings as a function of the shifted energy. The curves correspond to the radius of the ring, $R = 5M$ (solid line), $10M$ (dotted line), and $R = 25M$ (dashed line). The other parameters are fixed as the inclination angle, $i = 45^\circ$, and the black hole spin, $a = 0.998M$.

References

- Chandrasekhar S. 1960, Radiation Transfer (Dover, NY) p24, p234
- Chen K., Eardley D.M. 1991, ApJ 382, 125
- Connors P.A., Piran T., Stark R.F. 1980, ApJ 235, 224
- Dabrowski Y., Fabian A.C., Iwasawa K., Lasenby A.N., Reynolds C.S. 1997, MNRAS 288, L11
- Fabian A.C., Rees M.J., Stella L., White N.E. 1989, MNRAS 238, 729
- Iwasawa K., Fabian A.C., Reynolds C.S., Nandra K., Otani C., Inoue H., Hayashida K., Brandt W.N., et al. 1996, MNRAS 282, 1038
- Kojima Y. 1991, MNRAS 250, 629
- Laor A. 1991, ApJ 376, 90
- Laor A., Netzer H., Piran T. 1990, MNRAS 242, 560
- Nandra K., George I.M., Mushotzky R.F., Turner T.J., Yaqoob T. 1997, ApJ 477, 602
- Reynolds C.S., Young A.J., Begelman M.C., Fabian A.C. 1999, ApJ 514, 164
- Tanaka Y., Nandra K., Fabian A.C., Inoue H., Otani C., Dotani T., Hayashida K., Iwasawa K., et al. 1995, Nature 375, 659
- Weaver K.A., Yaqoob T. 1998, ApJ 502, L139

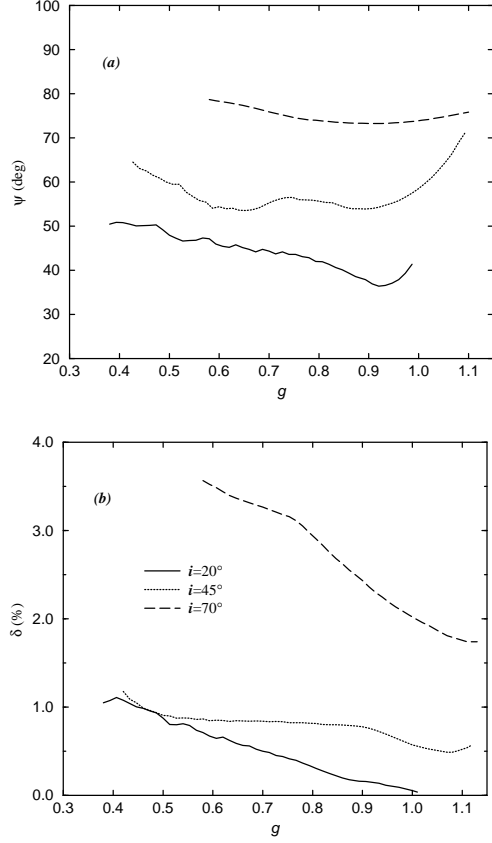


Fig. 2.. Effects of the inclination angle: (a) the angle and (b) degree of the polarization. Three curves are shown for $i = 20^\circ$ (solid line), $i = 45^\circ$ (dotted line), and $i = 70^\circ$ (dashed line). The other parameters are chosen as $R_{\text{in}} = 1.24M$ and $a = 0.998M$.

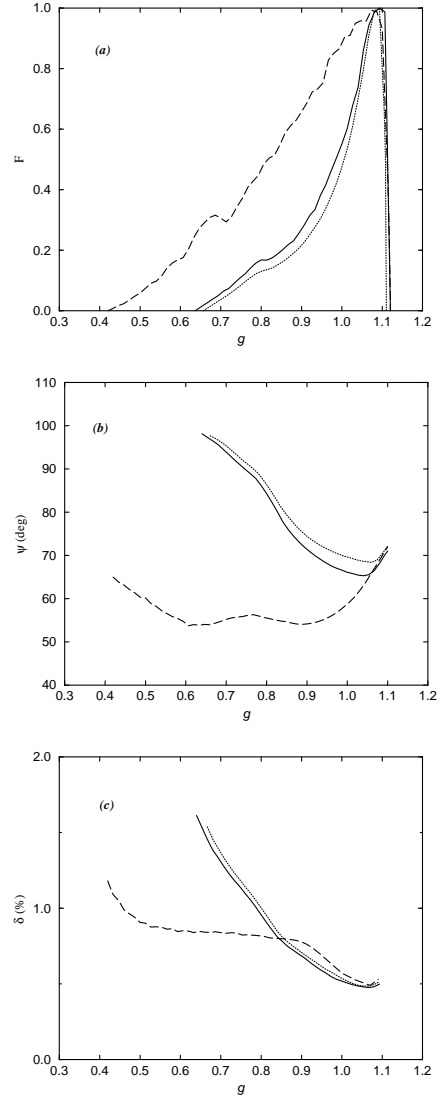


Fig. 3.. Effects of black hole spin on the emission lines: (a) line profile, (b) polarization angle, and (c) degree of polarization. The solid line is for the non-rotating case, i.e., $a = 0$, $R_{\text{in}} = 6M$. The dashed line is for the rotating case with $a = 0.998M$, $R_{\text{in}} = 1.24M$. We also show for a comparison the case of $a = 0.998M$, $R_{\text{in}} = 6M$ by the dotted line. The inclination angle is $i = 45^\circ$.

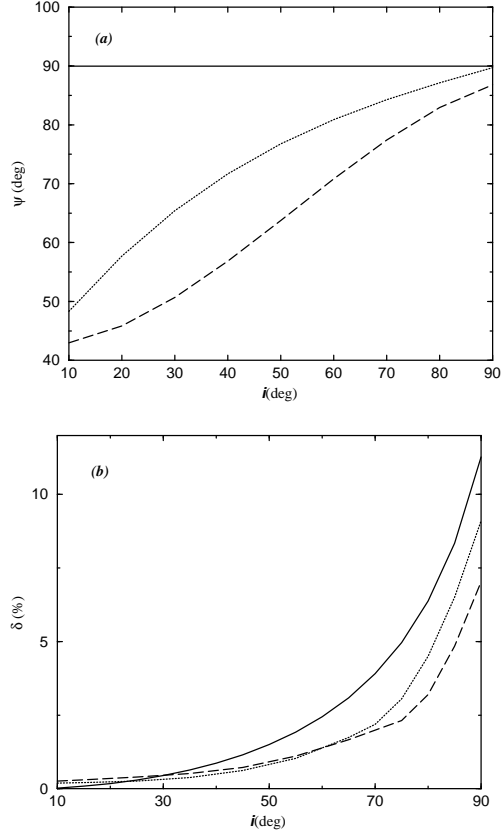


Fig. 4.. Polarization as a function of the disk inclination angle for the energy-integrated light: (a) the angle and (b) degree of the polarization. The non-relativistic calculation is shown by the solid line. Two models for the relativistic calculation are also shown. The dotted line corresponds to $a = 0$ and $R_{\text{in}} = 6M$, and the dashed line corresponds to $a = 0.998M$ and $R_{\text{in}} = 1.24M$.

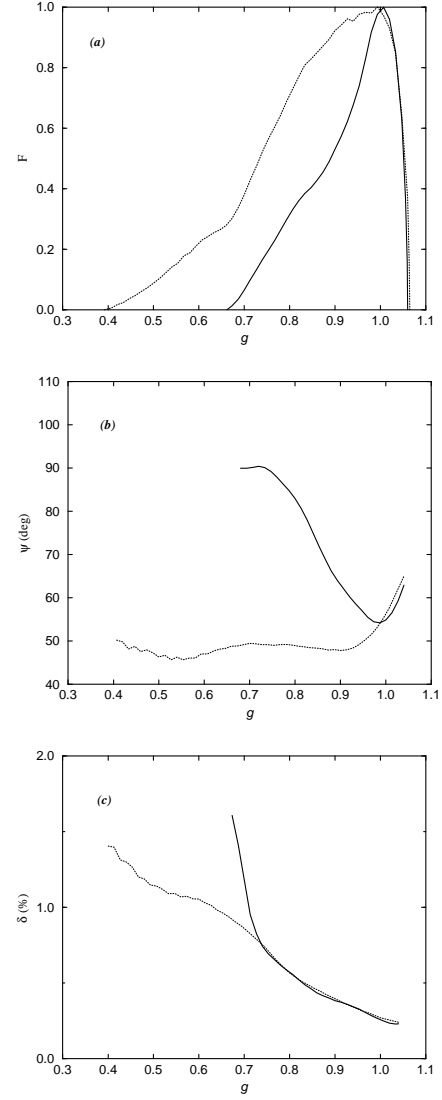


Fig. 5.. Application to the MCG-6-30-15: (a) line profile, (b) polarization angle, (c) percentage of polarization of the line. The adopted parameters of the solid line are $a = 0$, $R_{\text{in}} = 6M$, $R_{\text{out}} = 20M$, $q = 3$, and $i = 34^\circ$. The parameters of the dotted line are the same, except for $a = 0.998M$ and $R_{\text{in}} = 1.24M$.